MO-02 R04-53

PERMEATION BEHAVIOR AND PHYSICAL PROPERTIES OF NATURAL RUBBER NANOCOMPOSITES

Walter Zukas*, Michael Sennett, Elizabeth Welsh, Axel Rodriguez, and David Ziegler
U.S. Army Research, Development and Engineering Command
Natick Soldier Center, Natick, MA 01760

Paul Touchet
U.S. Army Research Laboratory
Aberdeen Proving Ground, MD 21005

ABSTRACT

Nanocomposites made by adding nanoparticle reinforcement to polymers have been demonstrated to have significantly enhanced properties at relatively low levels of added reinforcement. The observed properties have in some cases been attributed to the shape of the reinforcing particle. Nanoparticle additives with a variety of particle morphologies and compositions have become commercially available in recent years. A study was carried out to examine the effects of varying nanoparticle morphology and composition on the mechanical and barrier properties of polymer nanocomposites made with natural rubber (NR). NR compounds were prepared containing different nanoparticles including montmorillonite layered silicate (MLS) clay, exfoliated graphite nanoparticles (EGN), carbon nanotubes (CNT) and conventional carbon black (CB). The cure behavior and mechanical properties of the prepared nanocomposites were investigated. Barrier property testing included permeation of selected organic compounds utilizing a recently developed fully flooded surface method. The relationships between these properties and nanoparticle composition and morphology are presented.

1. INTRODUCTION

Researchers (Giannelis, 1996; Messersmith & Giannelis, 1995; Lebaron et al., 1999; Gilman et al., 1997; and Pinnavaia & Beall, 2000) have found that polymer composites containing small amounts of nanosize clay particles (silicates, e.g. montmorillonite) possess unusual mechanical properties relative to their parent materials. In addition, these hybrid materials were found in many cases to tolerate higher temperatures than traditional polymer/particle composites. Nanoparticle reinforcement increases the polymer-particle interfacial surface area by orders of magnitude relative to conventional reinforcing particle sizes. The increased surface area increases the volume fraction of polymer that may have decreased segmental motion due to surface pinning (formation of a constrained layer). It has been hypothesized that the polymer close to the particle surface has an effective shift in the polymer's glass transition temperature, leading to lower permeability and altered thermomechanical properties.

The incorporation of nanoscale clays (MLS) into polymeric matrices has been shown to yield improved barrier properties, increased mechanical properties, and better fire resistance properties, relative to the unfilled polymer. However, these materials typically require chemical treatments of the clays to provide the exfoliated dispersions that are critical to achieve the noted improved properties. Development of successful surface treatment of silicate nanoparticles is non-trivial, and must be specifically tailored to each polymer type.

Graphite is widely used as a filler to control electrical and thermal conductivity of normally non-conducting or poorly conducting materials, in addition to improving mechanical properties. However, there is a limit to improvement of these properties using natural or synthetic graphite in a flake or powder form due to particle size and morphological characteristics of the particles. Using nanoscale exfoliated particles, much better dispersion in polymeric matrix systems can be achieved. This is expected to lead to significant increases in thermal and electrical conductivity, mechanical properties, and chemical resistance in nanocomposites using these materials. Specific properties can be adjusted by filler content, matrix polymer type, and processing techniques.

A new process has been recently developed to produce nanoscale graphitic platelets through the exfoliation of monolithic graphite. These particles can be used as fillers in polymer composites, and hold the promise of improved material properties in several areas. These include mechanical properties, barrier properties, electrical properties and thermal stability. These nanoscale exfoliated graphite platelets may not require any pretreatment prior to processing, similar to conventional carbon blacks. They are also of lower density (20% or more) when compared to the silicates and thus result in lower density composites. In addition, graphite has electrical properties that the silicates do not,

which offers additional functionality in the target materials such as EMI shielding, electrostatic dissipation and potential signature management applications. Preliminary results with these materials incorporated into thermoplastics and elastomers were reported by Zukas et al., 2004; Fukushima et al., 2004; and Kalaitzidou et al., 2004. All noted increases in physical properties with the incorporation of EGN.

Extensive literature has reported the exceptional physical properties associated with CNTs. Their highly graphitic structure and very high aspect ratio (length to width) holds high promise for applications requiring unique electrical and mechanical properties. While somewhat expensive to produce, at this time, these materials were included in this study for their distinctive morphology and properties.

2. EXPERIMENTAL

Three different morphology carbon nanoparticles were utilized as reinforcements in this study: platelet EGN (mechanically comminuted graphite from Cornerstone Technologies, synthetic and natural graphites), multiwall CNT (CVD grown multi-wall from MER Corp.), and spherical CB (FEF N-330). A platelet MLS from Southern Clay (alkyl quaternary ammonium treated, Cloisite 25A) was also used.

Natural rubber formulations were mixed using the procedures outlined in ASTM D 3182 and using a recipe similar to ASTM D 3192 (see references). The ASTM recipe is shown in **Table 1** and expressed in units of parts per hundred (weight) rubber (phr). The formulations investigated in this study followed this recipe and used a SMR-CV60 pale crepe natural rubber, an N-330 carbon black, and Akrochem BBTS (N-tert-butyl-2 benzothioazole sulfenamide) in place of the benzothiazyl disulfide as the accelerator.

Table 1 ASTM D 3192 Natural Rubber Formulation in units of parts per hundred rubber (phr)

Natural Rubber	100.00
Stearic acid	3.00
Zinc oxide	5.00
Sulfur	2.50
Benzothiazyl disulfide	0.60
Carbon Black	50.00

Only variations in the filler type and level from this ASTM standard formulation were made in this study. The previously listed nanoparticulates were substituted for the CB in the ASTM formulation at 10 phr and 50 phr. A 10 phr CB formulation, an unfilled formulation, and mixed fillers of equal amounts of CB with EGN and CB with CNT were also prepared. The formulations prepared in this study are summarized in **Table 2**.

Table 2 Prepared natural rubber formulations.

FILLER	LEVELS (phr)
None	0
Carbon Black (CB)	10 & 50
Natural EGN	10 & 50
Synthetic EGN	10 & 50
CNT	10 & 50
MLS	10 & 50
CB & Natural EGN	25 each
CB & CNT	25 each

A variable speed two roll rubber-mixing mill (**Figure 1**) was used to prepare the formulations. The rolls are 3 inches in diameter and 8 inches wide and roll speeds of 32 RPM front and 40 RPM rear were used. The rolls were water cooled to assure the milling stock temperature did not exceed 50°C during preparation. The batch size prepared was 200 g. All ingredients were weighed with a 0.01 g accuracy.

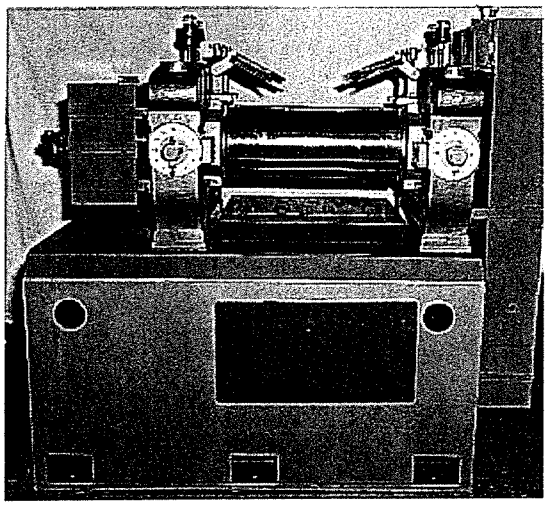

Figure 1. Two roll mill of the type used for preparation of the natural rubber formulations

Cure behavior of the compounded material was determined from the torque curve obtained with a Flexsys MDR 2000E Rheometer with a 0.5 degree arc and set nominally at 143°C. The scorch time was taken as the time required for the torque to show a 2 point rise from its initial minimum. The cure time was taken as the time required to reach 95% of the maximum torque.

Sheets of cured formulation were obtained by first sheeting out the compounded material with the roll mill to

a thickness slightly thicker than the mold cavity. The samples were then placed in preheated (143°C) molds in a 150 ton hydraulic press (24 inch by 24 inch platens) and pressure applied for the predetermined cure time at 143°C at a minimum of 500 psi on the total crossectional area of the cavity being molded. As soon as the curing period was completed, the press and mold were opened and the vulcanized sheet of rubber was removed from the mold, cooled in a water bath to room temperature, then dried.

The vulcanized samples were examined using both Scanning Electron Microscopy (SEM) and Transmission Electron Microscopy (TEM) to investigate both the surface features and internal dispersion of particles. The SEM was a Zeiss CSM 950 with images captured on Polaroid film then scanned to a computer. The TEM was a JEOL FasTEM 2010 with images captured on a 1 megapixel digital camera. The SEM and TEM sample preparation included washing the samples with a soap solution, to remove surface oils/dirt from handling. SEM specimens were coated with a 20nm thick application of Au/Pd from a Balzar's sputter coater. TEM samples were prepared by cryo-ultramicrotoming to 100nm thickness with a diamond knife on a Leica Ultracut with the cryogenic FCS attachment.

Mechanical testing was carried out using standard specimens cut from the prepared sheets on an Instron 5500R4302 instrument. Organic molecule penetration was measured with a liquid permeation cell and method developed at the Natick Soldier Center using an automated data collection system and a flame ionization detector (FID).

3. RESULTS AND DISCUSSION

The scorch time and established cure time data obtained for the samples investigated in this study are shown in **Table 3**. The scorch times were observed to be the most affected by the MLS and the least affected by the presence of EGN. The shorter scorch times indicate a strong accelerating affect by the MLS on the vulcanization reactions taking place. At 50 phr MLS, it was found necessary to reduce molding temperature to 138°C to slow the very rapid cure taking place to a controllable level.

SEM and TEM generally showed excellent dispersion of the CB, MLS, and CNT. The dispersion of the EGN containing samples, while good, did not match the dispersion of the other particles. Micron size pieces of EGN were still present within the samples and did not separate and disperse as individual sheets into the rubber. The excellent dispersion of the CNT at 50 phr is illustrated in **Figure 2** while the less than fully exfoliated graphite sheets are illustrated in **Figure 3** for an SEM of a sample of EGN at 10 phr in natural rubber.

Table 3 Cure behavior of natural rubber formulations

SAMPLE	SCORCH (min@143°C)	CURE (min@143°C)
No filler	12.53	26
10 phr CB	8.84	23
50 phr CB	5.80	23
10 phr EGN(nat)	11.48	26
50 phr EGN(nat)	10.23	27
10 phr EGN(syn)	11.90	29
10 phr CNT	11.62	27
50 phr CNT	6.61	20
25:25 phr CB:EGN(nat)	7.06	22
25:25 phr CB:CNT	6.36	22
10 phr MLS	4.22	16
50 phr MLS	1.67	9 (138°C)

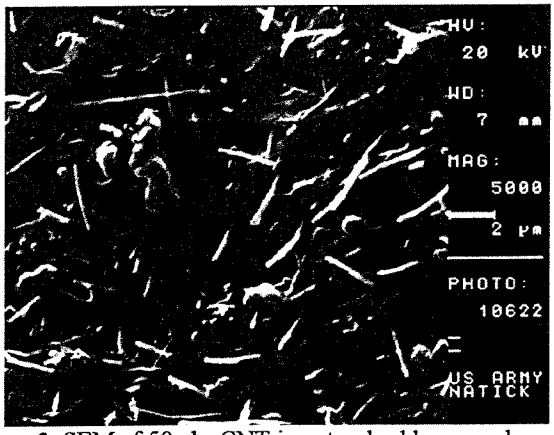

Figure 2 SEM of 50 phr CNT in natural rubber sample

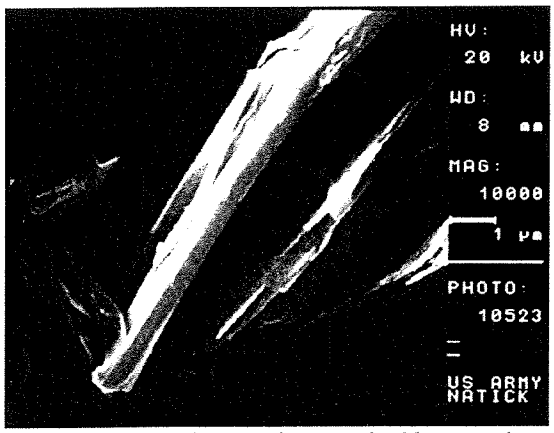

Figure 3 SEM of 10 phr EGN in natural rubber sample

Figure 4 illustrates the typical effect on mechanical tensile properties of adding carbon black to an elastomer formulation. These stress/strain curves show the unfilled, vulcanized formulation has a low Young's modulus and very high elongation to break (>1000%). Adding carbon black effectively "stiffens" the material, increasing Young's modulus, increasing the stress at break, and decreasing the elongation to break. The 50 phr level corresponds to a typical loading level for elastomer compounds in many applications (tires, etc.).

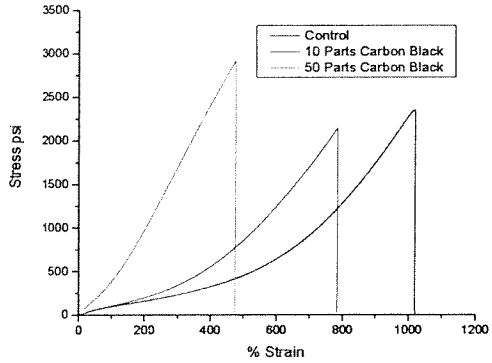

Figure 4 Stress/strain curves from Instron tensile testing of carbon black filled natural rubber samples.

The stress/strain tensile testing curves for MLS containing natural rubber formulations are shown in **Figure 5**. Similar to the CB curves shown in **Figure 4**, the addition of increasing amounts of MLS serves to decrease the elongation to break. Unlike the effect of CB, a significant increase in Young's modulus and stress to break is observed at the relatively low 10 phr of MLS. The 10 phr MLS actually had the highest stress to break of all samples tested, including all the samples at 50 phr filler. Addition of 50 phr MLS appeared to have a detrimental affect on tensile properties with significantly lower stress to break and elongation to break as shown in **Figure 5**.

In general, the carbon-based materials did not affect tensile properties to the same extent as the clay-based material at lower loading levels. This is illustrated in **Figure 6** for Young's modulus (at 2 to 4% strain) of the unfilled and 10 phr filled materials in this study. The EGNs did increase Young's modulus slightly more at this level than the carbon black, but not as much as the CNT and MLS. The MLS used in this study is chemically modified for compatibility with natural rubber. The EGN is not chemically modified and the microscopy results do indicate somewhat poorer dispersion as well. These are most likely the reasons for the lower values obtained when compared to the MLS. The relatively lower values for the CNT material when compared to the MLS was also surprising since the CNT has the theoretically highest modulus value of all the fillers utilized and was observed to be well dispersed. The orientation of the CNT was somewhat random with the test direction and the compatibility with the natural rubber was not optimized, both which may be reasons for lower than expected tensile properties.

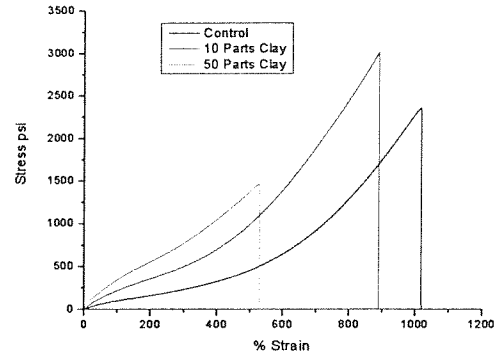

Figure 5 Stress/strain curves from Instron tensile testing of MLS filled natural rubber samples

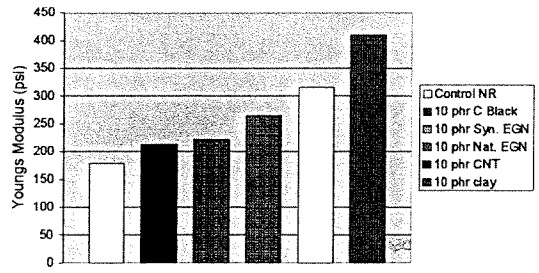

Figure 6 Nanocomposite Young's modulus for unfilled (Control) and various nanoparticles in natural rubber at 10 phr

The Young's modulus values (at 2 to 4% strain) for the 50 phr samples are shown in **Figure 7** along with the unfilled specimen. All fillers significantly increased this measure from the 10 phr value with the highest modulus obtained for the CNT filled specimen. The 25 phr mixtures (50 phr total) generally showed intermediate Young's modulus values when compared to the 50 phr single filler values. The standard carbon black formulation showed the lowest Young's modulus value when compared to all other formulations at 50 phr.

The permeation behavior of the natural rubber formulations was characterized utilizing a fully flooded surface cell, recently developed at Natick. A fully flooded

liquid challenge represents the most rigorous method for determining permeation. This simple, two-piece metal cell is shown in **Figure 8**. Circular specimens, 3 to 5 cm in diameter are clamped into the cell and a pool of liquid challenge is introduced on the top of the sample. The bottom of the sample is purged with an inert gas (typically nitrogen) to a flame ionization detector.

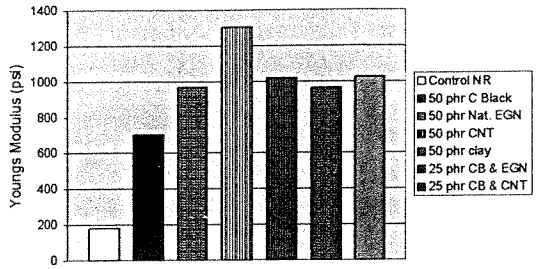

Figure 7 Nanocomposite Young's modulus for unfilled (Control) and various nanoparticles in natural rubber at 50 phr

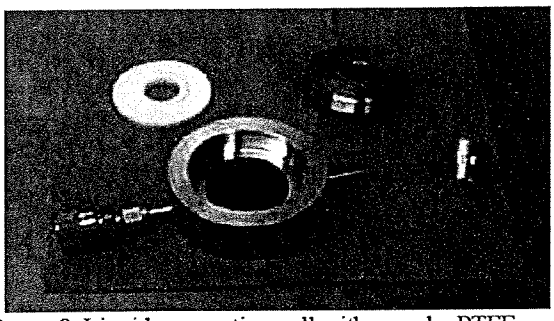

Figure 8 Liquid permeation cell with sample, PTFE gasket, threaded top, and cap.

Chemical warfare agent (CWA) simulants were used to mimic the permeation behavior of the actual CWA. Dichlorohexane (DCH) was used as a mustard simulant and diethylmethylphosphonate (DEMP) was used as a nerve agent simulant. The concentration of these were monitored with the FID as a function of time after introducing the liquid to the top of the sample.

A typical trace one obtains from this kind of permeation test is shown in **Figure 9**. Concentration is initially zero. The initial breakthrough of the liquid of interest is associated with the breakthrough time, T_b. The concentration then rises to an equilibrium flux value for the liquid, indicated by the plateau level at long times.

DEMP permeation curves for the 50 phr natural rubber samples are shown in **Figure 10**. The unfilled control clearly has the least resistance to this simulant with the earliest breakthrough time and highest equilibrium flux. The longest breathrough time was observed for the MLS filled sample. The shortest breakthrough time of the filled samples was associated with the CNT filled sample. The EGN filled material showed increased permeation resistance when compared to the carbon black filled sample, but was not as good as the MLS sample. The platelet morphology of both the MLS and EGN appears to lead to decreases in simulant permeation.

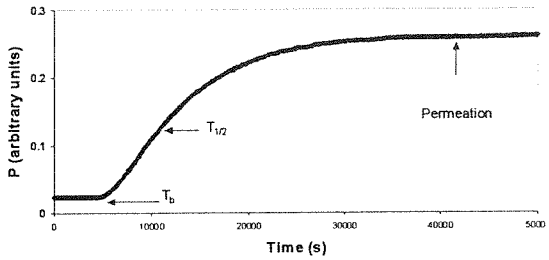

Figure 9 Typical liquid cell permeation curve

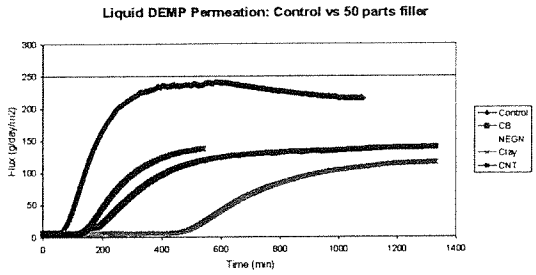

Figure 10 Liquid DEMP permeation in unfilled and 50 phr filled natural rubber formulations

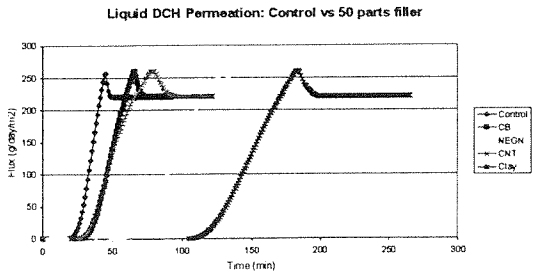

Figure 11 Liquid DCH permeation in unfilled and 50 phr filled natural rubber formulations

Similar observations were made for the permeation of DCH in the 50 phr natural rubber formulations (**Figure**

11) as for DEMP. The plateau value for flux in **Figure 11** is an artifact of the test procedure for this series of samples. The equilibrium flux of DCH actually exceeds the detector limit, so no substance should be placed on this value. However, the initial part of the curves does represent the concentration of DCH as a function of time.

Again, the unfilled material is the most permeable and the MLS the least. The EGN is clearly less permeable than the carbon black and CNT. Again, the platelet morphology of the MLS and EGN appear to decrease permeation in natural rubber formulations. The tubular morphology of the CNT and spherical geometry of the CB are not as effective barriers.

CONCLUSION

Nanocomposite morphology and surface chemistry have definitive effects on the nanocomposite properties of the natural rubber formulations prepared in this study. Increases in physical properties and barrier properties were observed with the introduction of both carbon and clay nanoparticles when compared to standard carbon black filled formulations. Good dispersion alone is not enough to ensure optimal reinforcement or barrier properties. The surface treated clays showed increased mechanical and barrier properties and better dispersion when compared to the untreated EGN materials. This demonstrates the critical role the interphase must play in nanocomposite behavior.

ACKNOWLEDGEMENTS

The authors wish to acknowledge Dr. JoAnn Ratto, Dr. Donald Rivin, and Dr. James Zheng at the Natick Soldier Center and Prof. Zhifeng Ren at Boston College for their assistance.

REFERENCES

ASTM D 3182 Standard, "Practice for Rubber – Materials, Equipment, and Procedures for Mixing Standard Compounds and Preparing Standard Vulcanized Sheets."

ASTM D 3192 Standard, "Standard Test Methods for Carbon Black Evaluation in NR (Natural Rubber)"

Fukushima, H., Lee, S., and Drzal, L., 2004: Graphite Platelet/Nylon Nanocomposites, *Proc. SPE ANTEC 2004*, 1441-1445.

Giannelis, E., 1996: Polymer Layered Silicate Nanocomposites, *Advanced Materials*, **8**, 29.

Gilman, J., Kashiwagi, T., and Lichtenhan, J., 1997: Nanocomposites: A Revolutionary New Flame Retardant Approach, *SAMPE Journal*, **33** 40.

Kalaitzidou, K., Fukushima, H., and Drzal, L., 2004: Mechanical and Electrical Properties of Exfoliated Graphite-Platelet Polypropylene Nanocomposites, *Proc. SPE ANTEC 2004*, 1533-1537.

Lebaron, P., Wang, Z., and Pinnavaia, T., 1999: Polymer-layered silicate Nanocomposites: An Overview, *Applied Clay Science*, **15**, 11.

Messersmith, P., and Giannelis, E.,1995: Synthesis and Barrier Properties of Poly(e-Caprolactone) – Layered Silicate Nanocomposites, *J. Polym. Sci. A*, **33**, 1047.

Pinnavaia, T. and Beall,, G., 2000: *Polymer Clay Nanocomposites*, Wiley, Chichester, England.

Zukas, W., Froio, D., Ratto, J., Rodriguez, A., Sennett, M., Thellen, C., Welsh, E., and Ziegler, D., 2004: Effects of Nanoparticle Morphology on the Permeation and Physical Properties of Polymer Nanocomposites, *Proc. SPE ANTEC 2004*, 2415-2419.